ARTICLES

Identification of stem cells in small intestine and colon by marker gene *Lgr5*

Nick Barker[1], Johan H. van Es[1], Jeroen Kuipers[1], Pekka Kujala[2], Maaike van den Born[1], Miranda Cozijnsen[1], Andrea Haegebarth[1], Jeroen Korving[1], Harry Begthel[1], Peter J. Peters[2] & Hans Clevers[1]

The intestinal epithelium is the most rapidly self-renewing tissue in adult mammals. It is currently believed that four to six crypt stem cells reside at the +4 position immediately above the Paneth cells in the small intestine; colon stem cells remain undefined. *Lgr5* (leucine-rich-repeat-containing G-protein-coupled receptor 5, also known as *Gpr49*) was selected from a panel of intestinal Wnt target genes for its restricted crypt expression. Here, using two knock-in alleles, we reveal exclusive expression of *Lgr5* in cycling columnar cells at the crypt base. In addition, *Lgr5* was expressed in rare cells in several other tissues. Using an inducible Cre knock-in allele and the *Rosa26-lacZ* reporter strain, lineage-tracing experiments were performed in adult mice. The Lgr5-positive crypt base columnar cell generated all epithelial lineages over a 60-day period, suggesting that it represents the stem cell of the small intestine and colon. The expression pattern of *Lgr5* suggests that it marks stem cells in multiple adult tissues and cancers.

The absorptive epithelium of the small intestine is ordered into crypts and villi[1], which in the mouse turn over every three to five days. The massive rate of cell production in the crypts is balanced by apoptosis at the tips of the villi. Until now, intestinal stem cells have not been functionally identified owing to the lack of unique markers and the absence of stem-cell assays. The analysis of mouse chimaeras and mutagen-induced somatic clones[2,3] as well as the study of regeneration after injury have allowed an operational definition of stem-cell characteristics. Self-renewing stem cells cycle steadily to produce the rapidly proliferating transit-amplifying cells capable of differentiating towards all lineages. The estimated number of stem cells is between four and six per crypt[2]. Long-term DNA-label retention has tentatively located stem cells at 'position +4' directly above the Paneth cells[4]. Three differentiated cell types (enterocytes, goblet cells and enteroendocrine cells) form from transit-amplifying cells at the crypt–villus junction and continue their migration in coherent bands stretching along the crypt–villus axis. Each villus receives cells from multiple different crypts. The fourth principal differentiated cell type, the Paneth cell, resides at the crypt bottom. The colon epithelium contains crypts, but has a flat surface rather than carrying villi. This epithelium comprises two main differentiated cell types: the absorptive colonocytes and the goblet cells[1]. Until now, no stem cells have been identified in the colon.

Lgr5 is expressed in crypt base columnar cells

Because Wnt signals constitute the principal driving force behind the biology of the crypt[5], we hypothesized that some Wnt target genes may be specifically expressed in the stem cells. We have previously described the Wnt target gene programme in human colorectal cancer cells and found that it is physiologically expressed in intestinal crypts[6,7]. Of approximately 80 selected Wnt target genes[7], most were expressed in either Paneth cells or transit-amplifying cells. The *LGR5* gene, however, was expressed in a unique fashion. It behaved as a Wnt target gene, because its expression was extinguished on the induced inhibition of Wnt pathway activity by dominant-negative TCF4 in a cell system described earlier[6] (Fig. 1a, lane 1 versus 2). Accordingly,

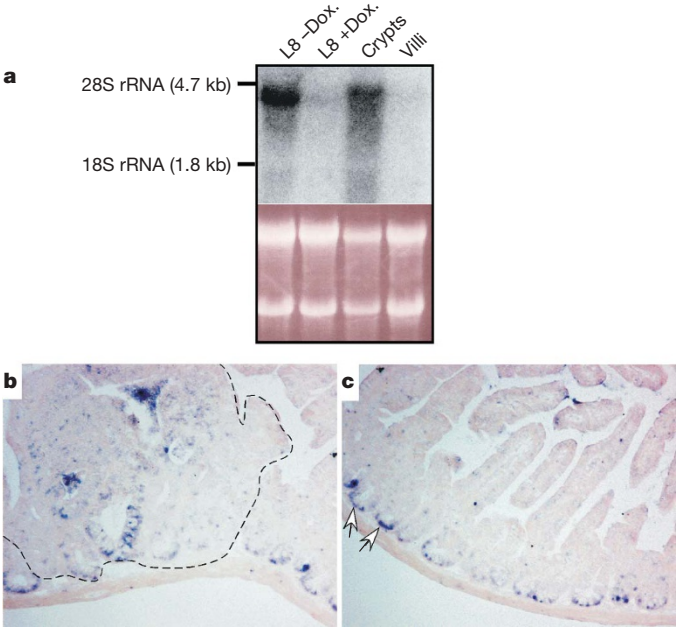

Figure 1 | *Lgr5* is a Wnt target gene in a human colon cancer cell line and is expressed in mouse crypts. **a**, Northern blot analysis (upper panel); ethidium-bromide-stained gel (lower panel). Lane 1: control Ls174T-L8 cells. Lane 2: Ls174T-L8 cells after 24-h doxycycline (Dox.)-induced Wnt pathway inhibition as in ref. 6. Note the strong downregulation of the 4.4-kilobase (kb) *Lgr5* messenger RNA on Wnt pathway inhibition. Lane 3: RNA extracted from isolated mouse small intestinal crypts, which unavoidably suffers from limited degradation resulting in some smearing. Lane 4: RNA extracted from isolated mouse villi. Note the specific expression of *Lgr5* in mouse crypts. **b**, **c**, Two overlapping images of an *in situ* hybridization performed on small intestines of an Apc^{Min} mouse, illustrating the ubiquitous expression of *Lgr5* at crypt bottoms (examples marked with white arrows) and the expression in the adenoma in **b** (marked by a dashed line).

[1]Hubrecht Institute, Uppsalalaan 8, 3584CT Utrecht, The Netherlands. [2]The Netherlands Cancer Institute, Antoni van Leeuwenhoek Hospital, Plesmanlaan 121, 1066 CX Amsterdam, The Netherlands.

the gene was expressed in the crypts, but not the villi, of mouse small intestine (Fig. 1a, lane 3 versus 4). *In situ* hybridization revealed expression in a limited number of cells located at all crypt bottoms as well as in adenomas in the small intestine of an Apc^{Min} (a mutant allele of *Apc* as present in multiple intestinal neoplasia (*Min*) mice) mouse (Fig. 1b, c). This expression pattern, enlarged in Fig. 2c, clearly differed from that obtained with a Paneth-cell-specific gene (Fig. 2a) or a transit-amplifying-specific gene (Fig. 2b). The *Lgr5* gene seemed to mark the cycling crypt base columnar (CBC) cells, interspersed between Paneth cells (Fig. 2d–h).

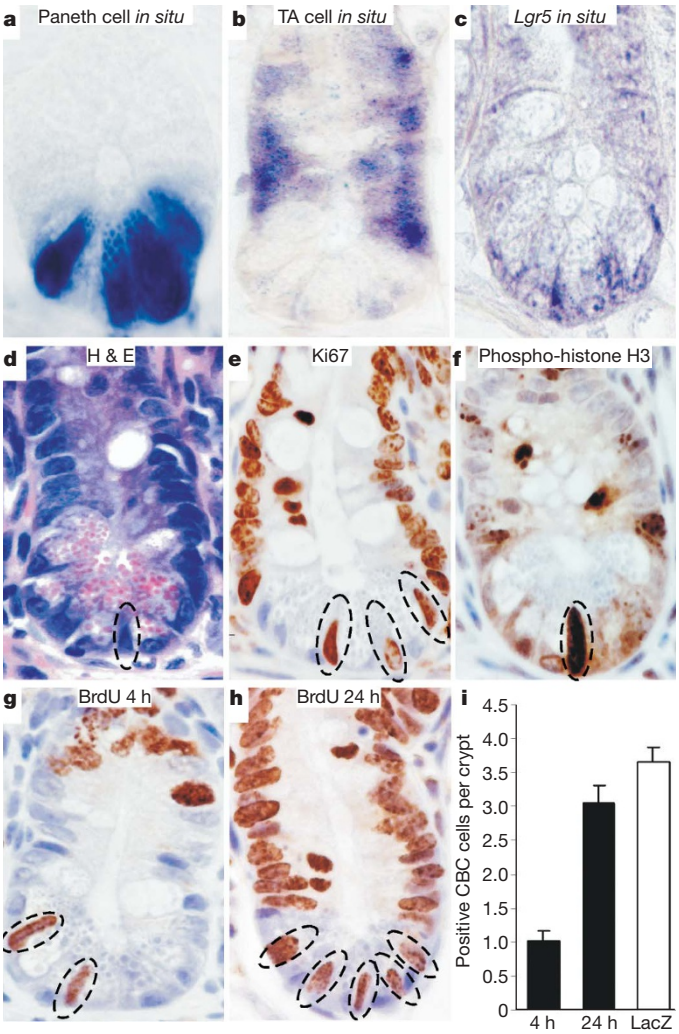

Figure 2 | *Lgr5* expression in cycling CBC cells of the small intestine. **a**–**c**, *In situ* hybridization was performed with probes specific for three Tcf target genes demonstrating non-overlapping expression patterns on the crypt epithelium. **a**, *Defa1* (also known as *Cryptdin1*) specifically marks Paneth cells at the crypt base; **b**, *Wdr43* (also known as *KIAA0007*) marks the transit-amplifying cells located above the Paneth cells; **c**, *Lgr5* is specifically expressed in 4–8 cells intermingled with the Paneth cells at the crypt base. All sense controls were negative (not shown). **d**, CBC cells (circled) are only poorly visible on haematoxylin and eosin (H&E)-stained sections. **e**, CBC cells (circled) are $Ki67^{+}$. **f**, Some CBC cells express the M-phase marker phospho-histone H3 (circled). **g**, BrdU incorporation in CBC cells 4 h after a single dose of BrdU (circled). **h**, BrdU incorporation in CBC cells after 24 h continuous BrdU labelling (circled). **i**, Quantification of BrdU-labelled and LacZ-positive CBC cells per crypt. Four independent stretches of proximal small intestine totalling 400 crypts were counted. Results are depicted as means and standard deviations of numbers of positive CBC cells per crypt. The black bars show numbers of BrdU-positive CBC cells per crypt section after 4 h or 24 h; the white bar shows total number of CBC cells per crypt section assessed by counting LacZ-positive cells in *Lgr5-lacZ* mice.

Lgr5 encodes an orphan G-protein-coupled receptor, characterized by a large leucine-rich extracellular domain[8]. *Lgr5* was on our original list of Wnt targets in colorectal cancer[6], but has since been observed in ovarian and hepatocellular carcinomas[9,10]. To study its expression in detail, we obtained a knock-in allele, in which *lacZ*, preceded by an internal ribosome entry site (*IRES*), is integrated just amino-terminal to the first transmembrane domain essentially creating a null allele (Fig. 3a).

The $Lgr5^{-/-}$ phenotype was described in ref. 11. A malformation of the tongue and lower jaw causes newborn mutants to swallow air, leading to their death soon after birth. We observed the same phenotype. Of note, crypts and intestinal stem cells are first established several weeks after birth[12]. The generation of heterozygous *Lgr5-lacZ* mice allowed us to detail the expression of *Lgr5*. Before birth, a dynamic and complex expression pattern was observed (N. Barker *et al.*, manuscript in preparation). Around birth, *Lgr5* expression subsided in virtually all tissues. Expression in adult mice was restricted to rare, scattered cells in the eye, brain, hair follicle, mammary gland, reproductive organs, stomach and intestinal tract (Fig. 3, and not shown). In the small intestine, *Lgr5* expression was observed in slender cells at the bottom of small intestinal (Fig. 3b, c) and colon (Fig. 3d, e) crypts. Counting of blue cells in small-intestinal crypts

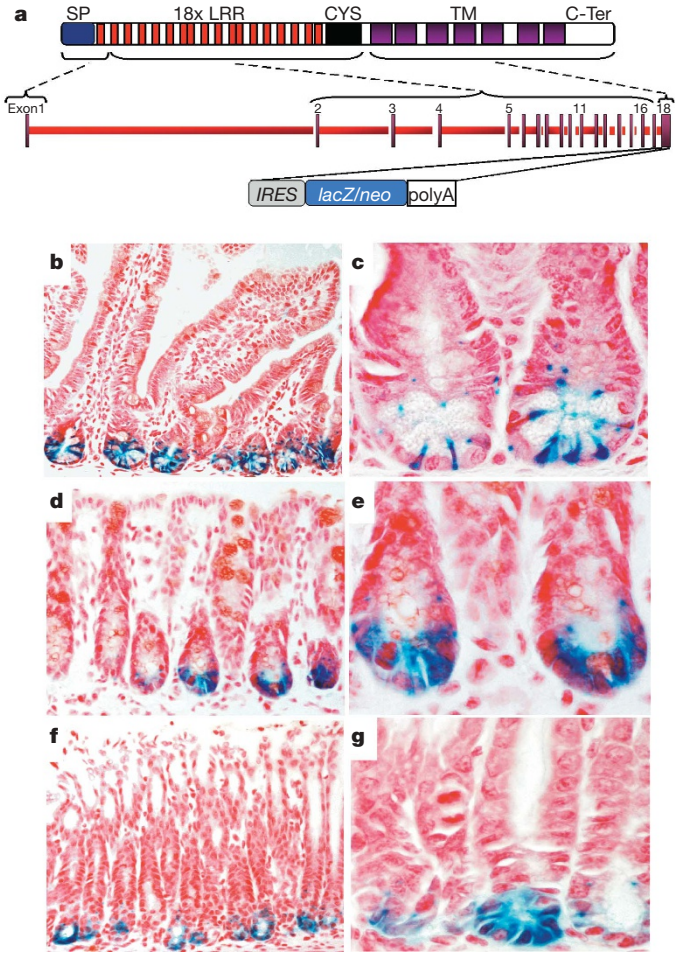

Figure 3 | Restricted expression of an *Lgr5-lacZ* reporter gene in adult mice. **a**, Generation of mice carrying *lacZ* integrated into the last exon of the *Lgr5* gene, removing all transmembrane (TM) regions of the encoded Lgr5 protein. Neo, neomycin resistance cassette; SP, signal peptide; LRR, leucine-rich repeat region; C-Ter is carboxy terminus. **b**–**h**, Expression of Lgr5-LacZ (blue) in selected adult mouse tissues. **b**, **c**, In the small intestine, expression is restricted to six to eight slender cells intermingled with the Paneth cells at the crypt base. **d**, **e**, In the colon, expression is confined to a few cells located at the crypt base. **f**, **g**, Expression in the stomach is limited to the base of the glands.

sectioned through the lumen revealed the presence of approximately 3.5 of such cells per sectioned crypt (Fig. 2i, white bar). More than 30 yr ago, ref. 13 noted the presence of cycling cells between the Paneth cells; these were named 'crypt base columnar' cells. It has been proposed that these cells may harbour stem-cell activity[2,14,15].

Lgr5$^+$ CBC cells are actively cycling

By morphology, the slender Lgr5$^+$ CBC cells with their scant cytoplasm and wedge-shaped nuclei pointing towards the crypt lumen were readily distinguishable from the adjacent Paneth cells. The CBC cells were frequently positive for the proliferation marker Ki67 (Fig. 2e and Supplementary Fig. 1) and also occasionally expressed the M-phase marker phospho-histone H3, indicating that the cells are typically cycling (Fig. 2f). Indeed, a 4-h pulse of 5-bromodeoxyuridine (BrdU) labelled approximately one of these cells per crypt section (Fig. 2g and i, left black bar), whereas a 24-h continuous BrdU labelling resulted in more than three positive cells per crypt section (Fig. 2h and i, right black bar), close to the total number of CBC cells per crypt section (Fig. 2i, white bar). This observation implied that the average cycling time of CBC cells is in the order of one day.

Unique ultrastructural anatomy of Lgr5–EGFP$^+$ CBC cells

To visualize live CBC cells and to study their potential 'stemness', we generated another knock-in allele, by integrating an enhanced green fluorescent protein (*EGFP*)-*IRES-creERT2* cassette at the first ATG codon (Fig. 4a and Supplementary Fig. 2). Heterozygous mice were healthy and fertile. The GFP pattern observed in adult tissues faithfully recapitulated the pattern previously seen with the *Lgr5-lacZ* allele (data not shown, and Fig. 4). Confocal imaging allowed the visualization of the Lgr5$^+$ cells by GFP fluorescence in small intestine (Fig. 4b, c, e) and colon (Fig. 4f). A three-dimensional reconstruction of the crypt in Fig. 4e (Supplementary Movie 1) illustrated the wedge-like shape of the CBC cells. Immuno-electron microscopy using immunogold labelling of the GFP-positive CBC cells and of neighbouring Paneth cells and fibroblasts illustrated the unique ultrastructural anatomy of the CBC cells (Fig. 4g, h). Typically, the CBC cells were relatively broad at their base, contained a flat, wedge-shaped nucleus and scarce organelles. A slender extension of apical cytoplasm was squeezed in-between neighbouring endoplasmic-reticulum- and granule-rich Paneth cells, extended to the crypt lumen and carried some apical microvilli.

We then crossed the *EGFP-IRES-creERT2* knock-in allele with the Cre-activatable *Rosa26-lacZ* reporter[16] (Fig. 4a). Injection of tamoxifen activates the CreERT2 fusion enzyme in *Lgr5*-expressing cells. Cre-mediated excision of the roadblock sequence in the *Rosa26-lacZ* reporter should then irreversibly mark Lgr5$^+$ cells. Moreover, although potential progeny of these cells will no longer express GFP, the activated *lacZ* reporter should act as a genetic marker, facilitating lineage tracing.

Lgr5$^+$ CBC cells are distinct from the +4 cells

Expression of *lacZ* was not observed in non-induced mice (not shown). To visualize in the crypts the location of CBC cells in which the latent Cre enzyme could be activated by tamoxifen, we treated 2–3-month-old mice with tamoxifen and killed the mice 12-h later. As evident in Fig. 5a, blue LacZ signals appeared at the typical CBC positions. We determined the frequency at which the blue cells appeared at specific positions relative to the crypt bottom, according to the scheme in Fig. 5b. Most of the Cre$^+$, LacZ-labelled CBC cells occurred at positions between the Paneth cells, whereas only 10% of these cells were observed at the +4 position (Fig. 5b, blue line). Quantitative data on the position of long-term DNA-label-retaining cells obtained in adult mice after irradiation (marking the '+4' intestinal stem cell) were published recently[17]. Comparison of these data (Fig. 5b, red line) with the position of CBC cells harbouring activatable Cre revealed that the two markers identified largely non-overlapping cell populations.

Another defining characteristic of the +4 cells is their exquisite sensitivity to low-dose (<1 Gy) radiation[4]. To compare relative radiation sensitivity between CBC cells and +4 cells, adult mice were irradiated with 1 Gy or 10 Gy and were killed 6 h later at the peak of apoptosis. Active caspase-3-positive cells were visualized by immunohistochemistry (Supplementary Fig. 3a). The frequency of caspase-3-positive cells per crypt was determined by counting

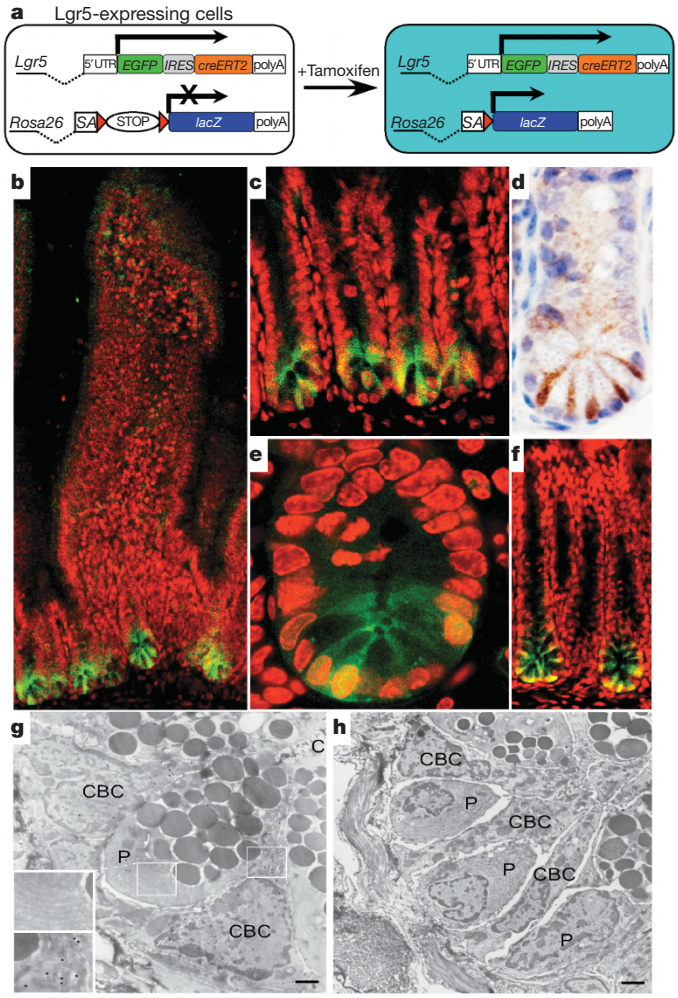

Figure 4 | EGFP expression in an *Lgr5-EGFP-IRES-creERT2* knock-in mouse faithfully reproduces the *Lgr5-lacZ* expression pattern in the intestinal tract. **a**, Generation of mice expressing EGFP and *creERT2* from a single bicistronic message by gene knock-in into the first exon of *Lgr5*. SA, splice acceptor; UTR, untranslated region. **b**, **c**, **e**, Confocal GFP imaging counterstained with the red DNA dye ToPro-3 confirms that *Lgr5* expression is restricted to the six to eight slender cells sandwiched between the Paneth cells at the crypt base of the small intestine. **b**, The entire crypt–villus unit; **c**, enlargement of crypt regions; **d**, immunohistochemical analysis of EGFP expression in intestinal crypts. **e**, Two-dimensional image of three-dimensional reconstruction (Supplementary Movie 1 and Supplementary Fig. 2). **f**, Confocal imaging of EGFP expression in the colon confirms that *Lgr5* expression is restricted to a few cells located at the crypt base. **g**, Cryo-electron microscopy section of crypt stained for GFP with immunogold (scale bar, 1,000 nm). Quantification of specificity of labelling: gold particles were counted over 255 μm^2 of CBC cell cytosol (1,113 particles), 261 μm^2 of Paneth cell cytosol (305 particles) and 257 μm^2 of fibroblast cytosol (263 particles) outside the crypt. Thus, CBC cytoplasm had 4.36 gold particles per μm^2; in contrast, the Paneth cells had 1.17 gold particles per μm^2 and the fibroblast control had 1.02 gold particles per μm^2. C, crypt lumen; P, Paneth cells. **h**, Unlabelled cryo-electron microscopy section (scale bar, 2,000 nm), underscoring the ultrastructural characteristics of CBC cells and their positions relative to Paneth cells.

apoptotic cells in three classes: CBC cells (defined by their location between the Paneth cells), +4 cells (located directly above the Paneth cells) and transit-amplifying cells (located at position 5–15, Supplementary Fig. 3b). Maximal apoptosis at the +4 position was already reached at 1 Gy (Supplementary Fig. 3a, upper panel, black arrows) in concordance with ref. 4, whereas 10 Gy caused significantly more apoptosis than 1-Gy irradiation in CBC (Supplementary Fig. 3a, lower panel, white arrows) and transit-amplifying cells, confirming the different identities of the CBC and +4 cells.

Lgr5$^+$ CBC cells are the small intestinal stem cells

Adult mice were then subjected to a tamoxifen pulse and were killed at 1 day (Fig. 5c), 5 days (Fig. 5d), 12 days, 35 days (not shown) and 60 days after induction (Fig. 5e and Supplementary Fig. 4). One day after induction, occasional CBC cells in small intestine and colon

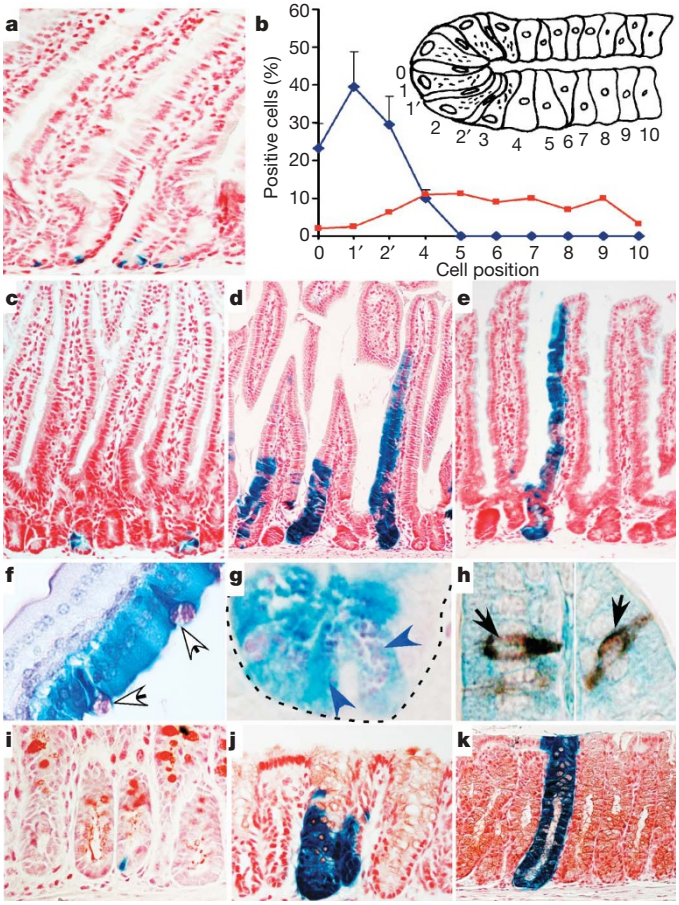

Figure 5 | Lineage tracing in the small intestine and colon. a, *Lgr5-EGFP-IRES-creERT2* knock-in mouse crossed with *Rosa26-lacZ* reporter mice 12 h after tamoxifen injection. **b**, Frequency at which the blue cells appeared at specific positions relative to the crypt bottom, according to the scheme in the inset. Results are depicted as means and standard deviations of four independent stretches of proximal small intestine totalling 400 positive crypts. Most of the Cre$^+$ LacZ-labelled CBC cells occurred at positions between the Paneth cells, whereas only 10% of these cells were observed at the +4 position directly above the cells (blue line). Quantitative data on the position of long-term DNA-label-retaining cells obtained in adult mice after irradiation (marking the '+4' intestinal stem cell) were published recently[17]. The graph shows a comparison of these data (red line) with the position of CBC cells carrying activated Cre. **c–e**, Histological analysis of LacZ activity in small intestine 1 day after induction (**c**), 5 days after induction (**d**) and 60 days after induction (**e**). **f–h**, Double-labelling of LacZ-stained intestine using PAS demonstrates the presence of goblet cells (**f**, white arrows) and Paneth cells (**g**, blue arrows) in induced blue clones. Double-labelling with synaptophysin demonstrates the presence of enteroendocrine cells within the induced blue clones (**h**, black arrows). **i–k**, Histological analysis of LacZ activity in colon 1 day after induction (**i**), 5 days after induction (**j**) and 60 days after induction (**k**).

expressed LacZ (Fig. 5c, i). As is demonstrated for whole-mount small intestine in Supplementary Fig. 4, parallel ribbons of cells emanated from the crypt bottoms and ran up the side of adjacent villi at later time points. For each of the time points, 200 crypts were counted in the proximal small intestine to determine the percentage containing blue cells. After 1 day, 5 days, 35 days and 60 days, these numbers were 22%, 39%, 25% and 36%, respectively. Thus, all CBC cells seemed capable of long-term maintenance of the self-renewing epithelium.

Double-labelling of 60-d-induced intestine revealed Periodic-Acid-Schiff (PAS)-positive goblet cells (Fig. 5f), PAS-positive Paneth cells (Fig. 5g) and synaptophysin-positive enteroendocrine cells (Fig. 5h) in the LacZ-stained clones. Using mutational marking, ref. 2 reported the existence of different types of long-lived epithelial clones; that is, columnar (enterocyte) clones, mucous (goblet) clones and mixed clones. Our clones were exclusively of the mixed variety. In blue clones, the frequency of goblet cells (114 of 2,043 total cells counted), enterocytes (1,846 of 2,043) and Paneth cells (83 of 2,043) was comparable to the frequency of goblet cells (127 of 3,691 total cells counted), enterocytes (3,345 of 3,691) and Paneth cells (127 of 3,691) in unmarked adjacent epithelium. As noted[2], the third secretory cell type, the enteroendocrine cell, was too rare to allow accurate enumeration. Taken together, we conclude that the Lgr5$^+$ CBC cells represent the genuine stem cells of the small intestine.

Lgr5$^+$ cells are the stem cells of the colon

Analysis of the colon yielded essentially identical observations. The Lgr5$^+$ cells yielded blue clones emanating from the crypt bottom (Fig. 5i). These clones contained colonocytes as well as goblet cells, and essentially remained unchanged during the 60 days of chase (Fig. 5j, k). One important difference to the situation in the small intestine involved the kinetics of clone formation. At 5 days, blue staining in most crypts was still restricted to the bottom, and entirely blue crypts were only rarely observed, implying that the colon stem cells were more often quiescent than their small-intestinal counterparts. At later days, the relative number of entirely blue crypts increased. Lgr5$^+$ colon cells fulfilled the stem-cell requirements in being pluripotent and capable of maintaining epithelial self-renewal over long periods of time.

Our observations provide the definitive characterization of the intestinal stem cell by lineage tracing using the expression of a single marker gene, *Lgr5*. The small intestinal Lgr5$^+$ cells are generally not quiescent, but are rapidly cycling, as demonstrated by the expression of Ki67 and phospho-histone H3, by the incorporation of BrdU and by the kinetics of ribbon formation. Lgr5$^+$ cells of the small intestine seem to divide more actively than their colonic counterparts, probably reflecting differences in the rate of epithelial turnover between the two organs. It seems counterintuitive that stem cells cycle. This is, however, not unprecedented. Germ stem cells in the *Drosophila* testis and ovary, arguably the best understood adult stem cells in animals, cycle throughout the lifetime of the adult fly[18]. Similarly, a recent elegant study demonstrated that adult stem cells of mammalian skin are continuously cycling[19].

The cycling +4 cells have previously been proposed to represent the small intestinal stem cells[4], a notion not confirmed here. This proposal was based on the observation that a DNA label incorporated during periods of high stem-cell activity was specifically retained in cells at the +4 position. Long-term label retention is often used as an indirect strategy to identify stem cells[12]. It should be noted, however, that terminally differentiating cells will also retain DNA labels, and that label retention should therefore be interpreted with caution. Previous studies have proposed other markers for intestinal stem cells. Musashi[20,21] and CD133 (ref. 22) in our hands stain up to 30–50 cells per crypt (not shown), which seem to encompass CBC cells as well as early transit-amplifying cells. Reference 23 described several molecular markers for the +4 cells, including phospho-PTEN, phospho-AKT and 14-3-3ζ. Our current study implies that the validity of these putative stem-cell markers should be reconsidered.

Lgr5 may mark stem cells in other adult tissues

It seems rather unique that adult stem cells can be identified on the basis of the expression of a single gene. This phenomenon may not be restricted to the intestine, because we observe highly restricted *Lgr5* expression in a variety of other tissues. Indeed, *Lgr5* was recently reported to be the second most highly upregulated gene as assessed by differential expression arraying on isolated hair follicle stem cells[24]. Moreover, preliminary lineage tracing experiments in the hair follicle support the notion that $Lgr5^+$ cells represent stem cells (N. Barker, H. Clevers and R. Toftgard, unpublished data). Whereas patterns of proliferation in stomach glands have indicated that the epithelial stem cells reside at the isthmus, halfway between the gland base and epithelial surface[25], we find *Lgr5* expressed at gland bottoms (Fig. 3f, g). Ongoing lineage tracing experiments imply that the entire glands derive from these cells (N. Barker and H. Clevers, unpublished data). In the mammary gland, stem cells reside in the basal epithelial layer[26], where we observe *Lgr5* expression (not shown). Lgr5 may thus represent a more general marker of adult stem cells. If true, the mouse models developed in the course of this study will allow the isolation as well as specific genetic modification of live adult stem cells in a variety of organs. We first identified *Lgr5* as a gene expressed in colon cancer cells[6]. It is expressed in other cancers[9,10] and, as described in the current study, is also in scattered cells in pre-malignant mouse adenomas. Future studies should explore the possibility that these $Lgr5^+$ malignant cells may represent cancer stem cells.

METHODS SUMMARY

Northern blotting and induced Wnt pathway inhibition in LS174T clone L8. This was performed as in ref. 6. Crypt and villus epithelial preparations for RNA isolation were generated from 1–2-cm lengths of intestine by 8 rounds of incubation in a solution containing phosphate-buffered-saline lacking Ca^{2+} and Mg^{2+} (PBS0), 1 mM EDTA and 1 mM EGTA at 4 °C for 10 min, followed by vigorous shaking. Fractions 3–4 and 7–8, comprising predominantly villi and crypts, respectively, were used for RNA isolation.

Mice. *Lgr5-lacZ* mice were generated by homologous recombination in embryonic stem cells targeting an *IRES-lacZ* cassette to the 5′ end of the last exon, essentially removing all transmembrane regions (Lexicon). *Lgr5-EGFP-IRES-creERT2* mice were generated by homologous recombination in embryonic stem cells targeting an *EGFP-IRES-creERT2* cassette to the ATG of *Lgr5*. *Rosa26-lacZ* Cre-reporter mice were obtained from the Jackson Laboratory.

Tamoxifen induction. Mice of >8 weeks were injected intraperitoneally with 200 µl tamoxifen in sunflower oil at 10 mg ml^{-1}.

BrdU injection. Mice were injected intraperitoneally at 4-h intervals with 200 µl BrdU solution in PBS at 5 mg ml^{-1}.

Tissue preparation for immunohistochemistry, *in situ* hybridization and LacZ analysis. This was performed as previously described[27]. *In situ* probes comprising a 1 kb N-terminal fragment of mouse *Lgr5* were generated from Image Clone 30873333. Antibodies: Ki67 antibody (Monosan), phosphohistone H3 (Campro Scientific), anti-synaptophysin (Dako) and anti-BrdU (Roche). Polyclonal rabbit anti-GFP was supplied by E. Cuppen.

Immuno-electron microscopy. Intestines were dissected and perfuse-fixed in 4% paraformaldehyde (PFA) in 0.2 M PHEM buffer (240 mM PIPES, 40 mM EGTA, 100 mM HEPES, 8 mM $MgCl_2$ pH 6.9), embedded in gelatine, cryosectioned with a Leica FCS cryoultratome and immunolabelled with polyclonal rabbit anti-GFP antibody. Samples were trimmed using a diamond Cryotrim 90 knife at –100 °C (Diatome), and ultrathin sections of 70 nm were cut at –120 °C using a Cryoimmuno knife (Diatome). For the low-magnification electron-microscope images, the 15-nm protein A-gold particles (UMCU) were briefly silver-enhanced with R-GENT SE-EM (Aurion)[28]. Aspecific binding was diminished by applying blocking solution (Aurion) before the primary antibody.

Full Methods and any associated references are available in the online version of the paper at www.nature.com/nature.

Received 21 June; accepted 24 August 2007.
Published online 14 October 2007.

1. Gregorieff, A. & Clevers, H. Wnt signaling in the intestinal epithelium: from endoderm to cancer. *Genes Dev.* **19,** 877–890 (2005).
2. Bjerknes, M. & Cheng, H. Clonal analysis of mouse intestinal epithelial progenitors. *Gastroenterology* **116,** 7–14 (1999).
3. Winton, D. J. & Ponder, B. A. Stem-cell organization in mouse small intestine. *Proc. Biol. Sci.* **241,** 13–18 (1990).
4. Potten, C. S., Booth, C. & Pritchard, D. M. The intestinal epithelial stem cell: the mucosal governor. *Int. J. Exp. Pathol.* **78,** 219–243 (1997).
5. Korinek, V. *et al.* Depletion of epithelial stem-cell compartments in the small intestine of mice lacking Tcf-4. *Nature Genet.* **19,** 379–383 (1998).
6. van de Wetering, M. *et al.* The β-catenin/TCF-4 complex imposes a crypt progenitor phenotype on colorectal cancer cells. *Cell* **111,** 241–250 (2002).
7. Van der Flier, L. G. *et al.* The intestinal Wnt/TCF signature. *Gastroenterology* **132,** 628–632 (2007).
8. Hsu, S. Y., Liang, S. G. & Hsueh, A. J. Characterization of two LGR genes homologous to gonadotropin and thyrotropin receptors with extracellular leucine-rich repeats and a G protein-coupled, seven-transmembrane region. *Mol. Endocrinol.* **12,** 1830–1845 (1998).
9. McClanahan, T. *et al.* Identification of overexpression of orphan G protein-coupled receptor GPR49 in human colon and ovarian primary tumors. *Cancer Biol. Ther.* **5,** 419–426 (2006).
10. Yamamoto, Y. *et al.* Overexpression of orphan G-protein-coupled receptor, *Gpr49*, in human hepatocellular carcinomas with β-catenin mutations. *Hepatology* **37,** 528–533 (2003).
11. Morita, H. *et al.* Neonatal lethality of LGR5 null mice is associated with ankyloglossia and gastrointestinal distension. *Mol. Cell. Biol.* **24,** 9736–9743 (2004).
12. Reya, T. & Clevers, H. Wnt signalling in stem cells and cancer. *Nature* **434,** 843–850 (2005).
13. Cheng, H. & Leblond, C. P. Origin, differentiation and renewal of the four main epithelial cell types in the mouse small intestine. V. Unitarian Theory of the origin of the four epithelial cell types. *Am. J. Anat.* **141,** 537–561 (1974).
14. Bjerknes, M. & Cheng, H. The stem-cell zone of the small intestinal epithelium. III. Evidence from columnar, enteroendocrine, and mucous cells in the adult mouse. *Am. J. Anat.* **160,** 77–91 (1981).
15. Stappenbeck, T. S., Mills, J. C. & Gordon, J. I. Molecular features of adult mouse small intestinal epithelial progenitors. *Proc. Natl Acad. Sci. USA* **100,** 1004–1009 (2003).
16. Soriano, P. Generalized *lacZ* expression with the ROSA26 Cre reporter strain. *Nature Genet.* **21,** 70–71 (1999).
17. Potten, C. S., Owen, G. & Booth, D. Intestinal stem cells protect their genome by selective segregation of template DNA strands. *J. Cell Sci.* **115,** 2381–2388 (2002).
18. Ohlstein, B., Kai, T., Decotto, E. & Spradling, A. The stem cell niche: theme and variations. *Curr. Opin. Cell Biol.* **16,** 693–699 (2004).
19. Clayton, E. *et al.* A single type of progenitor cell maintains normal epidermis. *Nature* **446,** 185–189 (2007).
20. Nishimura, S., Wakabayashi, N., Toyoda, K., Kashima, K. & Mitsufuji, S. Expression of Musashi-1 in human normal colon crypt cells: a possible stem cell marker of human colon epithelium. *Dig. Dis. Sci.* **48,** 1523–1529 (2003).
21. Potten, C. S. *et al.* Identification of a putative intestinal stem cell and early lineage marker; musashi-1. *Differentiation* **71,** 28–41 (2003).
22. O'Brien, C. A., Pollett, A., Gallinger, S. & Dick, J. E. A human colon cancer cell capable of initiating tumour growth in immunodeficient mice. *Nature* **445,** 106–110 (2007).
23. He, X. C. *et al.* BMP signaling inhibits intestinal stem cell self-renewal through suppression of Wnt–β-catenin signaling. *Nature Genet.* **36,** 1117–1121 (2004).
24. Morris, R. J. *et al.* Capturing and profiling adult hair follicle stem cells. *Nature Biotechnol.* **22,** 411–417 (2004).
25. Bjerknes, M. & Cheng, H. Multipotential stem cells in adult mouse gastric epithelium. *Am. J. Physiol. Gastrointest. Liver Physiol.* **283,** G767–G777 (2002).
26. Sleeman, K. E. *et al.* Dissociation of estrogen receptor expression and *in vivo* stem cell activity in the mammary gland. *J. Cell Biol.* **176,** 19–26 (2007).
27. Muncan, V. *et al.* Rapid loss of intestinal crypts upon conditional deletion of the Wnt/Tcf-4 target gene c-Myc. *Mol. Cell. Biol.* **26,** 8418–8426 (2006).
28. Peters, P. J., Bos, E. & Griekspoor, A. in *Current Protocols in Cell Biology* 4.7.1–4.7.9 (Wiley, New York, 2006).

Supplementary Information is linked to the online version of the paper at www.nature.com/nature.

Acknowledgements We thank R. Vries for preparing total RNA from isolated intestinal crypt and villus fractions and S. van den Brink for help with the embryonic stem cell work. We would like to acknowledge financial support from the following sources: Genmab B.V., Koninklijke Nederlandse Akademie van Wetenschappen (KNAW), Koningin Wilhelmina Fonds (KWF), Maag Lever en Darm Stichting (MLDS), European Molecular Biology Organization (EMBO), SenterNovem BSIK, Louis Jeantet Foundation and the European Union.

Author Information Reprints and permissions information is available at www.nature.com/reprints. The authors declare competing financial interests: details accompany the full-text HTML version of the paper at www.nature.com/nature. Correspondence and requests for materials should be addressed to H.C. (clevers@niob.knaw.nl).

METHODS

Generation of *Lgr5-EGFP-IRES-creERT2* mice. The expression construct was generated by cloning the various components into the polylinker of pBluescript SK+ (Stratagene) as depicted in Supplementary Fig. 2. Lgr5 flanking arms were generated by high-fidelity polymerase chain reaction from 129S7-derived genomic BAC clones. All components were sequence-verified. The expression construct (100 μg) was linearized and transfected into male 129/Ola-derived IB10 embryonic stem cells (provided by The Netherlands Cancer Institute) by electroporation (800 V, 3 μF). Recombinant embryonic stem cell clones expressing the neomycin gene were selected in medium supplemented with G418 (gentamycin sulphate; the effective concentration of which was determined by its kill curve) over a period of 7 days. Approximately 500 recombinant embryonic stem cell clones were picked into duplicate 96-well tissue culture plates and cultured to 70% confluency. One plate was cryo-preserved and the other plate was used for DNA isolation according to ref. 29. DNA from embryonic stem cells was screened for the presence of homologous recombinants by Southern blotting according to the strategy outlined in Supplementary Fig. 2. Positive clones were thawed, expanded into 6-well tissue-culture plates and injected into C57BL/6 blastocysts using standard procedures. Male chimaeras born after transplantation of the bastocysts into C57BL/6 foster mothers were subsequently mated with C57BL/6 females, and germline transmission was confirmed by screening offspring for the presence of the expression cassette in the *Lgr5* locus by polymerase chain reaction. The neomycin expression cassette was then excised *in vivo* by crossing the mice with EIIa-Cre mice as previously described[30].

β-galactosidase (LacZ) staining protocol. Organs were isolated and immediately incubated for 2 h in a 20-fold volume of ice-cold fixative (1% formaldehyde, 0.2% gluteraldehyde and 0.02% NP40 in PBS0) at 4 °C on a rolling platform. Intestines, colon and stomach were first cleaned by flushing with fixative to remove faeces and undigested food. The fixative was removed and the tissues washed twice in PBS0 for 20 min at room temperature (20 °C) on a rolling platform. The β-galactosidase substrate (5 mM $K_3FE(CN)_6$, 5 mM $K_4Fe(CN)_6{\cdot}3H_2O$, 2 mM $MgCl_2$, 0.02% NP40, 0.1% sodium deoxycholate and 1 mg ml^{-1} X-gal in PBS0) was then added and the tissues incubated in the dark overnight at room temperature. The substrate was removed and the tissues washed twice in PBS0 for 20 min at room temperature on a rolling platform. The tissues were then fixed overnight in a 20-fold volume of 4% PFA in PBS0 at 4 °C in the dark on a rolling platform. The PFA was removed and the tissues washed twice in PBS0 for 20 min at room temperature on a rolling platform.

The stained tissues were transferred to tissue cassettes and paraffin blocks prepared using standard methods. Tissue sections (4 μM) were prepared and counterstained with neutral red.

Whole-mount analysis of LacZ staining as shown in Supplementary Fig. 4 was performed on 150-μM tissue sections prepared on a vibratome (HM650V, Microm).

Confocal analysis of EGFP expression. 150-μm sections were prepared from non-fixed intestines using a vibratome and were fixed for 5 min in 4% formaldehyde. After counterstaining with ToPro-3 (Molecular Probes) the sections were analysed for EGFP expression by confocal microscopy (Leica SP2 AOBS). The observed emission spectrum was compared with reference spectra to confirm that the observed fluorescence was EGFP-derived.

***In situ* hybridization protocol.** The *in situ* probes used in this study correspond to expressed sequence tags obtained from the IMAGE consortium (Geneservice Ltd; ImaGenes GmbH). The GenBank accession and IMAGE numbers for these probes are as follow: mouse *Lgr5*, CN70148, IMAGE 30873333; Cryptdin-1, AA871421, IMAGE 1096215; and *KIAA0007*, BF158985, IMAGE 3982366. To ensure the specificity of the probes, we generated both sense and antisense probes by *in vitro* transcription using DIG RNA labelling mix (Roche) according to the manufacturer's instructions.

Intestines from normal or Apc^{Min} mice were flushed and fixed overnight in formalin. Samples were then dehydrated and embedded in paraffin, sectioned at 8 μM and processed for hybridization as described below. Sections were dewaxed, re-hydrated, treated with 0.2 M HCl, digested in proteinase K solution, post-fixed, treated in acetic anhydride solution and hybridized overnight for 24–48 h at 68 °C with various probes in 5× SSC (pH 4.5), 50% formamide, 2% blocking powder (Roche), 5 mM EDTA, 50 μg ml^{-1} yeast transfer RNA, 0.1% Tween 20, 0.05% CHAPS and 50 μg ml^{-1} heparin. Sections were then rinsed in 2× SSC and washed for 3 × 20 min at either 60 °C or 65 °C in 2× SSC per 50% formamide. After several rinses in Tris-buffered saline containing 0.05% Tween (TBST), sections were then blocked for 30 min in TBST containing 0.5% blocking powder (Roche). Sections were subsequently incubated in blocking solution overnight at 4 °C with alkaline phosphatase-conjugated anti-digoxigenin (1/2,000 dilution, Roche). After washing several times in TBST, the colour reaction was performed with NBT/BCIP solution. For image analysis, sections were temporally mounted in glycerol or permanently mounted after dehydration in Pertex.

Isolation of intestinal crypt and villus fractions. Intestines were washed in ice-cold PBS (Mg^{2+}/Ca^{2+}) and sliced longitudinally to expose the crypts and villi. The intestine was then cut into small pieces (1–2-cm long) and washed several times in ice-cold PBS (Mg^{2+}/Ca^{2+}) to remove contaminants such as faeces and hair. The intestine pieces were incubated in a solution containing PBS0 (lacking Mg^{2+}/Ca^{2+}), 1 mM EDTA and 1 mM EGTA at 4 °C for 10 min on a rotating platform. The PBS0, containing loose pieces of mesenchyme and intestine, was decanted, cold PBS0 was added, and the tube was shaken vigorously ten times. The cells shed into the PBS0 were collected and labelled as fraction 1. The intestine pieces were again incubated in solution containing fresh PBS0, 1 mM EDTA and 1 mM EGTA at 4 °C for 10 min on a rotating platform. The PBS0 was decanted, fresh PBS0 was added and the tube was shaken vigorously 10–15 times. The cells shed into the PBS0 were filtered through a 70 μM nylon cell strainer (BD Falcon) and the flow-through discarded. The tissue retained on the filter, comprising villi, was stored in PBS (Mg^{2+}/Ca^{2+}) on ice (fraction 2). The incubation, shaking and straining steps were repeated until eight fractions had been collected. Fractions 3–6 comprised pure villus tissue, whereas fractions 7 and 8 isolated as the flow-through from the cell strainer comprised pure crypt tissue.

29. Ramírez-Solis, R. *et al.* Genomic DNA microextraction: a method to screen numerous samples. *Anal. Biochem.* **201**, 331–335 (1992).
30. Lakso, M. *et al.* Efficient *in vivo* manipulation of mouse genomic sequences at the zygote stage. *Proc. Natl Acad. Sci. USA* **93**, 5860–5865 (1996).